A novel compensation method for polygonized mesa structures on (100) silicon substrate

Zhang Han(张涵)† and Li Weihua(李伟华)

(Key Laboratory of MEMS of the Ministry of Education, Southeast University, Nanjing 210096, China)

Abstract: A theoretical compensation method for polygonized mesa structures on (100) silicon substrate during the anisotropic etching process has been developed, which contains four stages as follows: prepare the information of the etching condition; predict the structure's undercutting profile; construct the topological structure of compensation patterns; and generate practical compensation patterns from the topological structure. The reasoning process is clearly stated, and detailed steps for the undercutting prediction and topological structure construction are summarized. Conclusions are also drawn about the rules which must be obeyed during the pattern generation process. The simulation and experimental results of some polygon structures are finally given to prove this method's validity and reliability.

Key words: (100) substrate; compensation method; polygonized mesa structure; simulation result; experimental result
DOI: 10.1088/1674-4926/31/6/063002 **PACC:** 0750 **EEACC:** 2575

1. Introduction

Silicon wet anisotropic etching with KOH solution is an important technology for bulk-micromachining. However, it causes undesired undercutting at most convex corners[1, 2]. As the structures of MEMS devices are becoming more and more ingenious, the impact of this defect is becoming more and more serious[1−4]. We expect a general method for generating suitable compensation patterns for any convex corner to offset the undesired erosion. However, the existing type of this method is mainly for rectangle structures[7, 11], and mostly concluded from experimental results[10, 11]. The lack of theoretical research will restrict the design patterns.

In this paper, we work on ⟨110⟩ edged (100) substrate with 30 wt% KOH solution at 70 ℃. According to the DFM (design for manufacture) theory[5, 6], the defect within prediction can always be prevented in advance. Hence, because the polygon structures are irregular and flexible, before the compensation method, we have to figure out the undercutting prediction method first. So, the realization process of the compensation for polygon structures consists of two main methods: the prediction method and the compensation method.

We divide the introduction paragraphs into three parts. In the first part, we will give a full theoretical description of the whole design method. A convenient way to determine the undercutting profile for the polygon structures has been concluded, which realizes the prediction by detailed border classification and accurate calculation. Moreover, the concept of topological field[12] is introduced to define the boundary of most compensation patterns. Also, the rules which must be obeyed during the practical compensation pattern generation process have been summarized. In the second part, we use square and octagon as examples to realize the method, and get the analysis results. In the last part, we verify the method by comparing the analysis results with the simulation results and the experimental results. Compared to the existing research findings, this method has extensive applicability and theoretical significance, and it is applicable for most polygon structures in the wet anisotropic etching process.

2. Method description

2.1. Stage one: preparation

Under our condition of ⟨110⟩ edged (110) silicon substrate with 30 wt% KOH solution, (311) emerges to be the fast-etching plane, and it meets the (100) substrate at the ⟨310⟩ direction. Meanwhile, the non-etching plane (111) meets the substrate at the ⟨110⟩ direction. The ⟨100⟩ direction is the intersecting line between different (100) planes[4, 7]. The first step for preparation is to find out the two-dimensional etching rates of all these intersecting lines.

As our object is the polygonized mesa structure, the borders' etching rates have to be taken into account. According to the conclusion of anisotropic etching simulation function[8, 9], another preparation step should be to figure out every border's etching rate for the destination structure.

2.2. Stage two: undercutting prediction

As we know, during the silicon anisotropic etching process, undercutting is always dominated by the fast-etching directions[4]. In addition, according to existing experimental results, the deformed structure under the same etching environment is doubtless[9]. Hence, the undercutting phenomenon must have its own theory.

In order to avoid the confusion of border erosion and corner undercutting, a square made of ⟨110⟩ directions becomes an ideal research model because the border's etching rate is considered to be zero. Combining the mechanism model of the anisotropic etching process and some experimental results, we arrive at the conclusion that the deformed corner must be the smallest obtuse corner which is larger than the original one at the same time[3, 4, 10]. Figure 1 shows all the possible undercutting directions around a ⟨110⟩ oriented square. For each corner,

† Corresponding author. Email: zhanghan_0719@163.com
Received 22 June 2009, revised manuscript received 15 January 2010

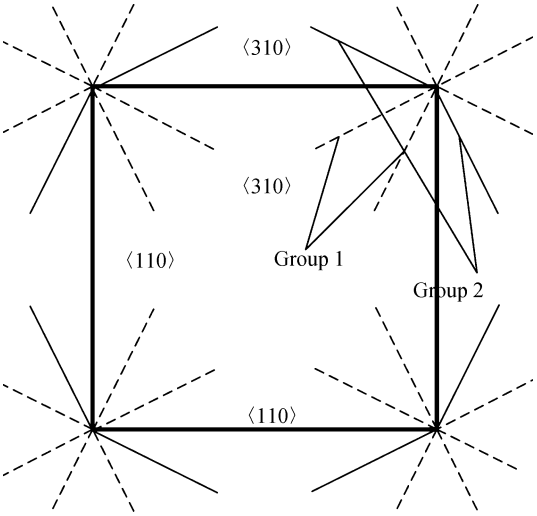

Fig. 1. ⟨310⟩ directions around a square.

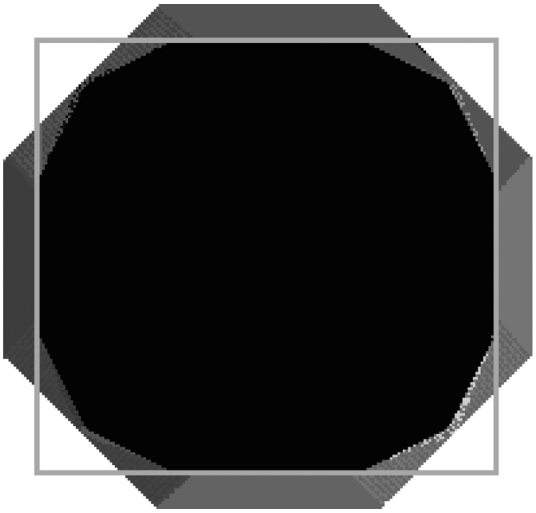

Fig. 2. Simulation result of a square.

it has only four ⟨310⟩ directions, which make up two groups. Apparently, with this restriction, the direction of group 1 will not emerge, because the angle is smaller than the target corner itself. The square will be only deformed by the direction of group 2. The analysis result is coincident with the simulation result shown in Fig. 2.

Now, we redraw the square and its undercutting directions in a ⟨110⟩ oriented coordinate system as shown in Fig. 3. Two diagonals and the coordinate system divide the plane into eight regions, and each region contains a border and its undercutting direction. The eight borders named from a to h cover all the borders' relative positions. So we link each position type with a unique ⟨310⟩ undercutting direction that is in the same one-eighth region. For any convex corner structure, as long as we classify each border's position type, we can easily know its relevant undercutting direction.

Although there are only eight kinds of border position, the practical convex corner can be countless. After the border classification, we have to reconsider that whether the borders and their undercutting directions meet the conclusion that "the deformed corner must be the smallest obtuse corner which is larger than the original one at the same time", and eliminate the directions which do not meet the cut. Figure 4 illuminates how the restriction works. We can see that the undercutting direction of border a is the only possible erosion path.

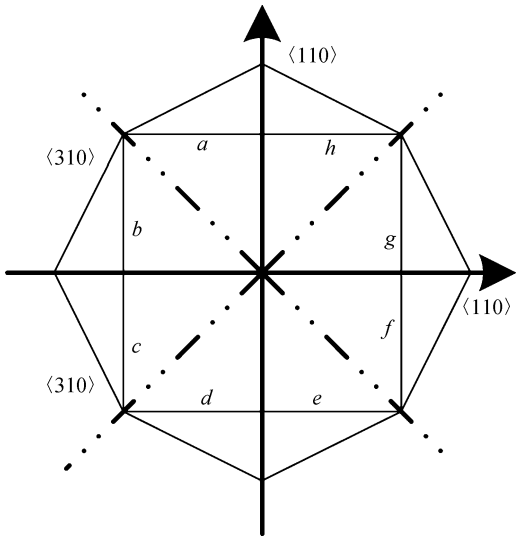

Fig. 3. Border classification.

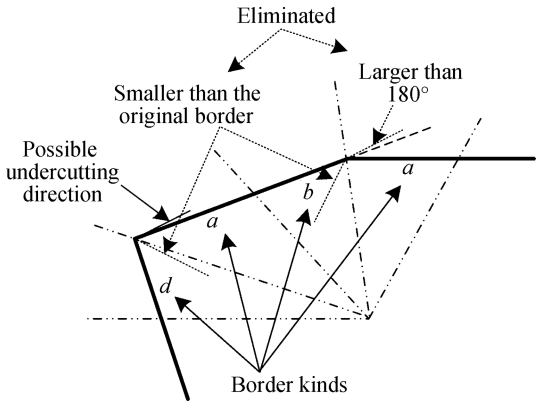

Fig. 4. Unqualified border elimination.

Finally, as most borders have etching rates, we need to discover their impact on the corner undercutting. For a corner with at least one possible undercutting direction, and on its undercutting direction side, we define the included angle between the border and its corner bisector as θ, and the included angle between the corner bisector and this border's undercutting direction is defined as α. Figure 5 displays the definition on an arbitrary corner A: $\angle\theta = \angle DAC$, $\angle\alpha = \angle DAF$. When they fulfill the relationship:

$$v_{\text{border}}/\sin\theta < v_{\langle 310\rangle}/\sin\alpha, \tag{1}$$

where v stands for velocity, the convex corner will be deformed at the undercutting direction on this border side. Otherwise, the corner will keep its shape and the borders will just etch parallel.

Clearly, by applying the analysis method above to every convex corner of a polygon structure, we could predict its whole deformed shape after the anisotropic etching process precisely.

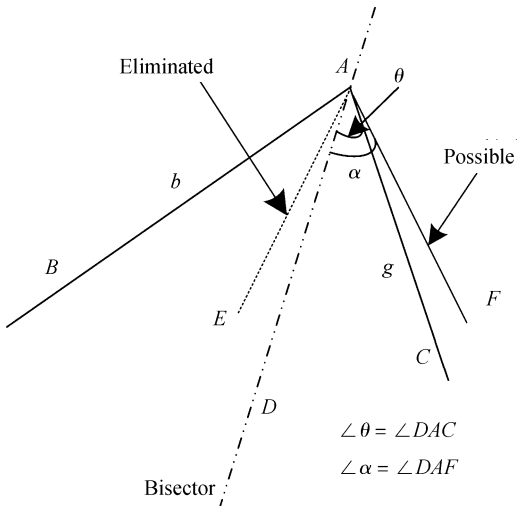

Fig. 5. Definitions of corners θ and α.

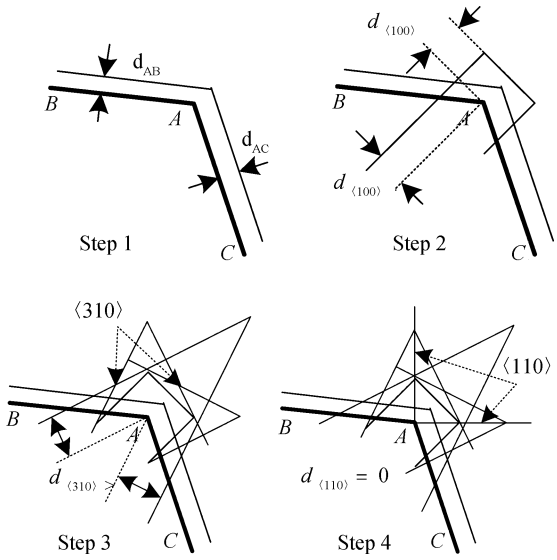

Fig. 6. Sketch of the topological construction process.

Therefore, we condense the prediction stage into four steps as:

(1) Classify every convex corner's border into a position type according to Fig. 3, and draw up each border's undercutting direction.

(2) Eliminate the undercutting directions which do not meet the conclusion that "the deformed corner must be the smallest obtuse corner which is larger than the original corner at the same time" as in Fig. 4.

(3) Figure out Eq. (1) with parameter values. The definitions of θ and α are supposed to be defined as in Fig. 5, while the borders' etching velocities have been determined in preparation step 2. If the calculation result of Eq. (1) is tenable, the corner will be deformed at its undercutting direction. Otherwise, the corner needs no corner compensation.

(4) Put every corner's undercutting prediction together to form a whole undercutting profile of the mask layout.

2.3. Stage three: topological structure construction

For a long time, convex corner compensation has been a key method to offset the undesired undercutting phenomenon. However, most of the existing compensation patterns lack theoretical reasoning, and compensation research is mainly concentrated on the rectangle structure[11]. Based on the detailed investigation of right-angled corner compensation[7], we find out that the essence of an ideal compensation pattern is to make the border or the border's undercutting direction reach the destination boundary as soon as the mesa structure reaches the designed depth. Hence, in the opposite way, by keeping these critical directions some certain distances away from the destination structure, we introduce the concept of topological structure to define the infancy frame for most compensation patterns.

Around the corner which will be deformed according to the prediction of section 2.2, the construction steps of the topological structure could be described as follows:

(1) Translate the polygon's borders with a nonzero etching rate outward at distance d_{border}. Make sure that:

$$d_{\text{border}}/v_{\text{border}} = H/v_{\langle 100\rangle}, \tag{2}$$

where H is the etching depth.

(2) Put all $\langle 100\rangle$ directions away from the destination corner apex at distance $d_{\langle 100\rangle}$, while:

$$d_{\langle 100\rangle}/v_{\langle 100\rangle} = H/v_{\langle 100\rangle}. \tag{3}$$

(3) Keep all the $\langle 310\rangle$ directions from the desired corner apex at distance $d_{\langle 310\rangle}$. The distance is supposed to fulfill the relationship:

$$d_{\langle 310\rangle}/v_{\langle 310\rangle} = H/v_{\langle 100\rangle}. \tag{4}$$

(4) Let the $\langle 110\rangle$ directions cross the destination corner apex, meaning:

$$d_{\langle 110\rangle} = 0. \tag{5}$$

Figure 6 takes an arbitrary corner as an example to display each step of this construction process separately to help understanding. Evidently, for a corner which will not be deformed, its topological structure can be constructed by step 1 only. The rest of the steps are meaningless as there is no need for corner compensation.

2.4. Stage four: practical compensation pattern generation

The topological structure just provides a basic frame for compensation design. The practical compensation patterns are generated by directly fitting some directions up or connecting some points with $\langle 110\rangle$ directions. Anyway, all the compensation patterns need to be coincident with the rules, which are summarized as follows according to the basic truth of the anisotropic etching process.

(1) Border compensation is prior to that of the corner.

(2) The apexes of the convex corners of the compensation structure, whose undercutting directions are chosen as the end-etching directions, should be on the topological boundary of their own undercutting directions.

(3) The angle of the convex corner defined in rule 2 should be smaller than that of the fast-etching direction.

(4) The profile of the compensation pattern cannot include any concave corners, unless they are made of two non-etching

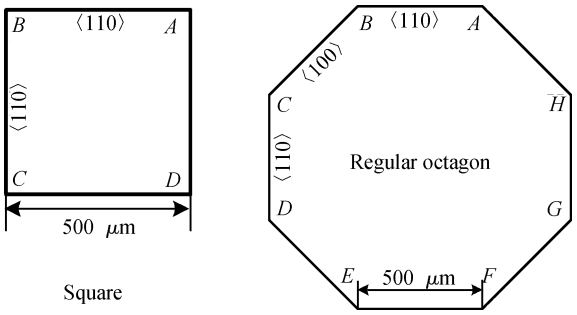

Fig. 7. Relative size of the square and regular octagon.

directions, or the concave corner is larger than the angle contained by any two of the non-etching directions, and meanwhile has one non-etching border.

3. Examples for verification

In this section, we apply the compensation method introduced above to a square and a regular octagon to test the method's applicability. The square is treated as a particular case of polygon structure here.

Figure 7 presents the two destination structures, and their final dimensions are designed to be 500 μm side length and 65 μm depth.

3.1. Preparation

Because the preparation work describes the characteristic parameters of the etching condition and the destination structures, we do the job for both of the two examples first.

Under our condition of ⟨110⟩ oriented (100) silicon substrate with 30% KOH solution at 70 ℃, the ⟨110⟩ direction is not etching. And the etching rates of ⟨100⟩ and ⟨310⟩ direction are considered as 1 μm/min and 1.484 μm/min separately[4, 7].

As we know, a square is made up of four ⟨110⟩ directions, and a regular octagon is made up of directions ⟨100⟩ and ⟨110⟩. So we can figure out each border's etching rate in Fig. 7.

3.2. Square

In section 2.2, we have already discussed the square's undercutting profile as shown in Figs. 2 and 3. Hence, we skip the prediction part and start with the topological structure construction stage directly.

By following the steps of section 2.3, we get the topological structure around the right-angled corner and name each direction as shown in Fig. 8. The distances of the corner apex to directions ⟨100⟩ and ⟨310⟩ are figured out to be 65 μm and 96.46 μm respectively.

By fitting up different directions and borders within the restriction of the pattern generation rules defined in section 2.4, we can get many practical compensation patterns. Here we present four sample structures which stand for four distinctive boundaries as shown in Fig. 9. Corner A selects line a and line b to make triangle compensation. By linking up the intersection points of line a and line c, line b and line e, as well as line d and line f with the ⟨110⟩ direction, we get the compensation pattern for corner B. Corner C illustrates the compensation with the non-etching direction ⟨110⟩ by using line c and

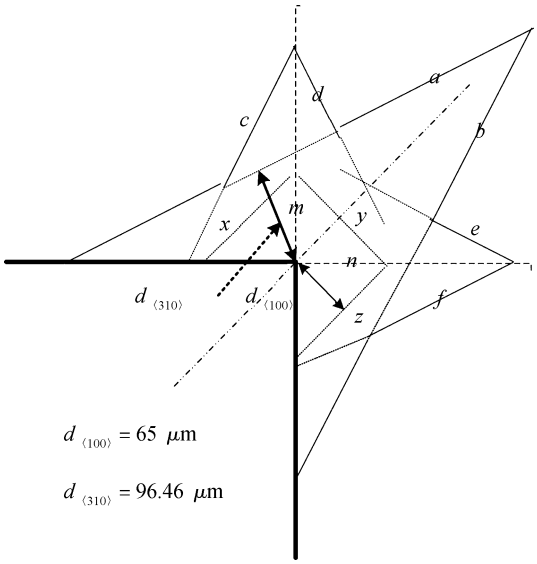

Fig. 8. Topological structure.

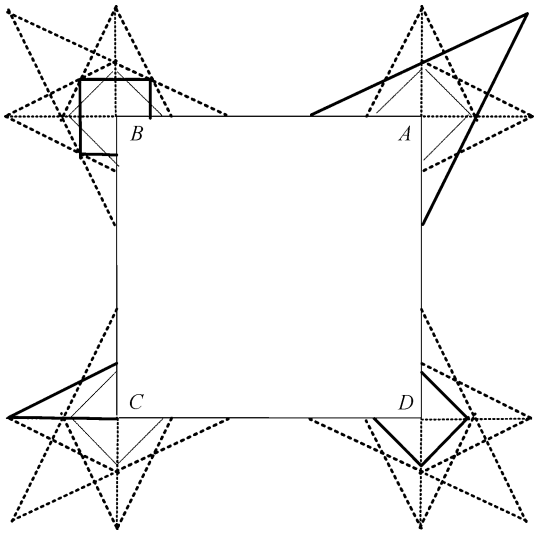

Fig. 9. Compensation patterns.

line m. The compensation of corner D is constituted with the ⟨100⟩ directions named x–z.

3.3. Regular octagon

A regular octagon has great symmetry. To determine its undercutting profile, we follow the steps of section 2.2. There are sixteen borders of eight convex corners in an octagon as divided by the two-dot chain lines. Figure 10 shows the border classification result and their undercutting directions. With the limitation of step 2 in stage 2, as well as the fact that the ⟨110⟩ direction's etching rate is 0, we forecast that undercutting only occurs at every corner's ⟨110⟩ side, and the ⟨100⟩ border will etch parallel.

According to the expectation, we follow the steps of stage 3 to form the topological structure. Because of the regular octagon's symmetry, Figure 11 only shows a quarter of it. Equally, $d_{\langle 110\rangle}$ and $d_{\langle 310\rangle}$ are still supposed to be 65 μm and 96.46 μm respectively. Abiding by the rules of stage four, Figure 12 shows four different compensation patterns generated

Table 1. Dimensions of the destination structures.

Polygon	Height (μm)	Side length (μm)	Distance (μm)		
			$d\langle 310\rangle$	$d\langle 110\rangle$	$d\langle 100\rangle$
Square Regular octagon	65	500	96.46	0	65

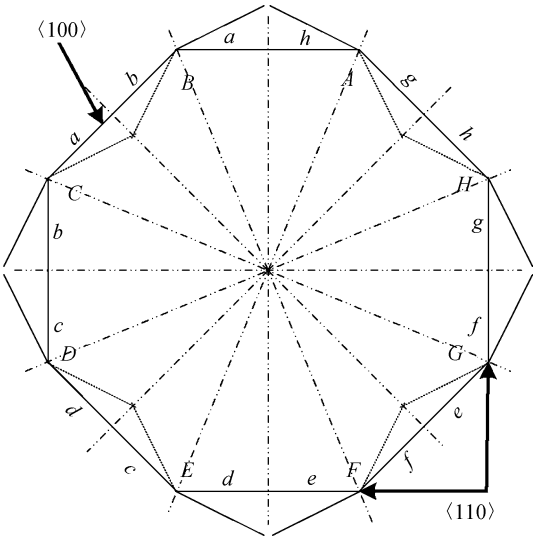

Fig. 10. Border classification.

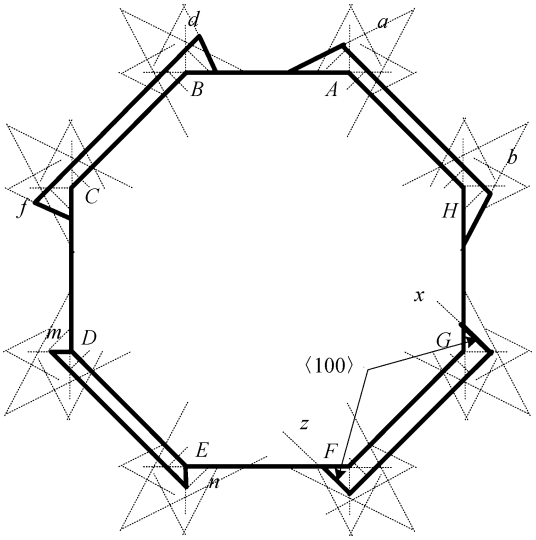

Fig. 12. Compensation patterns.

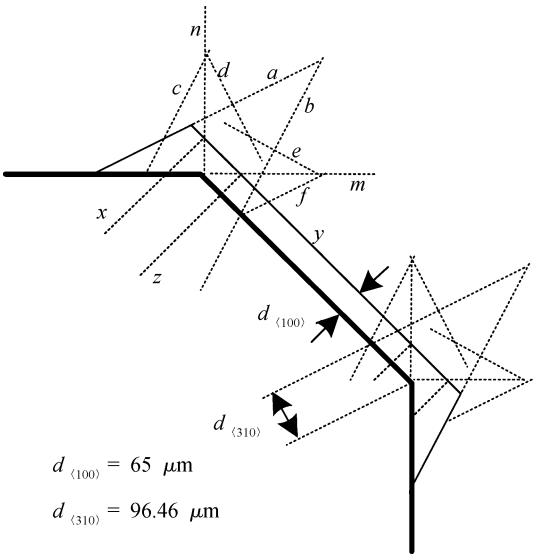

Fig. 11. Topological structure.

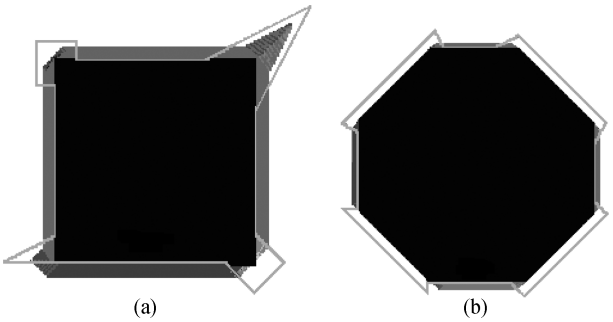

Fig. 13. Simulation results of the compensation patterns. (a) Square. (b) Regular octagon.

from Fig. 11. Since the border compensation is preferred and unique, the differences of the compensation patterns are told by the corner compensation part. The four couples of borders for corner compensation are chosen to be line a and line b, line d and line f, line m and line n, and line x and line z, and each couple represents a boundary kind.

4. Simulation and experimental results

So far, we have applied the compensation method to two polygon structures, and obtained some compensation patterns for them. Table 1 redisplays the dimensions of the destination structures and the key distances of their compensation patterns.

The simulation process for the mask layouts defined in Figs. 9 and 12 are carried out by the ACES (anisotropic crystalline etch simulation) tool. The simulation results are shown in Fig. 13.

From Fig. 13(a), it is clear to see that the compensation pattern on each corner is different, but all four right-angled corners are completely formed. Figure 13(b) illustrates four different compensation structures on one mask layout too. Obviously, these simulation results are coincident with our expectation. Corners and edges with compensation patterns are perfectly preserved.

We do the experiment under the given conditions, and the experimental results are collected as shown in Figs. 14 and 15. Figure 14(a) shows the mask layout on a square, and Figure 14(b) gives its etching results. It can be clearly seen that the surface of this square has been well protected, and the silicon shape left on the bottom is in agreement with the simulation re-

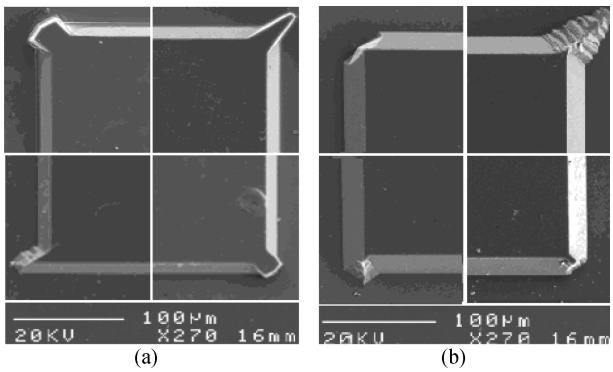

(a) (b)

Fig. 14. Experimental result for the square. (a) At the beginning of the etching. (b) At the end of the etching.

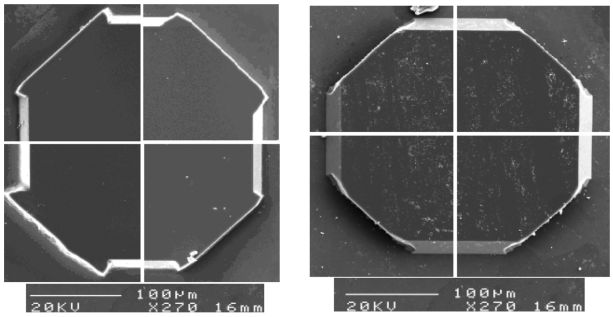

(a) (b)

Fig. 15. Experimental result for the octagon. (a) At the beginning of the etching. (b) At the end of the etching.

sult shown in Fig. 13(a). Equally, Figure 15(a) shows the mask layout of an octagon, just as shown in Fig. 12, and Figure 15(b) is the experimental result. Apparently, under the protection of these designed compensation masks, the two target structures are perfectly obtained. Both the simulation result and the experimental result prove the method's validity.

5. Conclusions

In this work, we present a novel method for generating suitable compensation patterns for polygonized mesa structures on (100) substrate. The method consists of four stages as follows: preparation stage for collecting basic information on the etching condition and the destination structure; prediction stage for identifying the undercutting profile of the structure to provide evidence for compensation design; construction stage for making a topological structure of practical compensation patterns; and final generation stage for transforming the topological structure to generate practical compensation patterns.

The method provides a theoretical system to deal with the mesa structures. It works very well on most polygon mesa structures. We take a square and a regular octagon as examples to deduce this whole method in this paper. Their simulation and experimental results verify the method's validity and applicability. Moreover, it fills up the blank field of polygon compensation, and offers much convenience for realizing DFM in the MEMS design process.

References

[1] Gabrie K J. Microelectromechanical systems. Proc IEEE, 1998, 86(8): 1534
[2] Pal P, Sato K, Gosalvez M A, et al. Novel wet anisotropic etching process for the realization of new shapes of silicon MEMS structures. International Symposium on Micro-NanoMechatronics and Human Science, 2007: 499
[3] Seidel H. The mechanism of anisotropic silicon etching and its relevance for micromachining. Tech Dig Transducers, Tokyo, Japan, 1987: 120
[4] Huang Q A. Silicon micromachining technology. Beijing: Science Publisher, 1996: 51
[5] White K P, Athay R N. Applying DFM in the semiconductor industry. Electronics Manufacturing Technology Symposium, 1995
[6] Sylvester D. Design for manufacturability: challenges and opportunities. 6th International Conference on ASIC, 2005, 1: 1169
[7] Guo T, Fan B, Guo H. Convex corner compensation in anisotropy etching on silicon (100). Nanotechnology and Precision Engineering, 2008, 6: 68
[8] Zhang P J, Huang Q A. Simulation of anisotropic etching of silicon based on MATLAB. Chinese Journal of Semiconductors, 2002, 23: 440
[9] Zhang P J, Huang Q A. Simulation of anisotropic etching-rate diagram for silicon. Research and Progress of SSE, 2002, 22: 89
[10] Jovic V, Lamovec J, Popovic M. Investigation of silicon anisotropic etching in alkaline solutions with propanol addition. 26th International Conference on Microelectronics, 2008
[11] Pal P, Sato K, Chandra S**.** Fabrication techniques of convex corners in a (100)-silicon wafer using bulk micromachining: a review. J Micromechan Microeng, 2007, 17: 111
[12] Zhang H, Li W. A novel method for generating a rectangular convex corner compensation structure in an anisotropic etching process. Journal of Semiconductors, 2009, 30(7): 073003